Materials and Structures (2025) 58:66
https://doi.org/10.1617/s11527-025-02586-0

ORIGINAL ARTICLE

Implementing the effect of geopolymer concrete pore solution pH in the standard rapid migration test NT Build 492 protocol

Yu Pang · Quang Dieu Nguyen · Arnaud Castel

Received: 7 May 2024 / Accepted: 24 January 2025 / Published online: 11 February 2025

Abstract This research investigates the impact of the pore solution pH values on chloride content at the colour change boundary determined according to the standard rapid migration test (NT Build 492), with a focus on alkali-activated materials, so-called geopolymer. The study investigates a range of geopolymer formulations using various proportions of ground granulated blast furnace slag (GGBFS), fly ash, and calcined clay, alongside different activator concentrations, to examine their influence on the pH value of the pore solution. Findings from this study suggest that the pH value of the pore solution greatly influence in the chloride ion concentration at the colour change boundary, which should be accounted for in the calculation of the non-steady-state migration coefficients (D_{nssm}). It is noted that mixtures with higher GGBFS content exhibit higher pH values than mixtures containing fly ash or calcined clay, impacting the D_{nssm}. The results advocate for modifications to the standard NT Build 492 protocol to enhance its applicability and accuracy for geopolymer materials, emphasizing the importance of using revised D_{nssm} values calculated considering the unique properties of geopolymer concrete for more durability assessment.

Y. Pang · Q. D. Nguyen (✉) · A. Castel
School of Civil and Environmental Engineering,
University of Technology Sydney (UTS), Sydney,
NSW 2007, Australia
e-mail: quangdieu.nguyen@uts.edu.au

Keywords Geopolymer · Alkali-activated materials · NT Build 492 · pH · Colour change boundary

1 Introduction

Concrete, a material widely recognised as the fundamental component of contemporary infrastructure, has played an essential role in the field of construction [1, 2]. Concrete's adaptability, durability, and cost-effectiveness have made it the preferred choice for a wide range of constructions, including tall skyscrapers and extensive motorways [3]. The concrete industry is currently confronted with a significant and urgent durability issue, namely the deterioration of concrete structures caused by the corrosion of reinforcement [4]. Reinforcement corrosion has the potential to undermine the structural soundness of concrete structures, resulting in premature failures and requiring expensive remediation or replacement [5, 6]. The understanding and mitigation of steel corrosion in concrete infrastructure worldwide is a matter of utmost significance [7].

The corrosion process, proposed by Tuutti, consists of two stages: initiation stage and propagation stage [8]. In chloride environments, the initiation stage describes the diffusion of chloride ions through the concrete pore structure toward the steel-concrete interface. The propagation stage begins when the critical chloride threshold is reached at the steel-concrete interface [9, 10]. Chloride concentration exceeding the critical chloride threshold triggers reinforcement corrosion, resulting in the formation and expansion of corrosion products, loss of bond strength, concrete cracking and spalling [11–13]. The propagation stage of chloride-induced corrosion significantly compromises the structural integrity of reinforced concrete. This degradation has a substantial effect on the ability of the structure to withstand loads and its overall lifespan [14, 15]. The rapid migration test (NT Build 492) is a standard test used to evaluate the chloride diffusion in the initiation stage [16]. The non-steady-state chloride migration coefficient (D_{nssm}) is calculated, based on the depth of chloride penetration determined by spraying silver nitrate 0.1M solution on the surface of freshly split concrete specimens. However, this chloride penetration depth so-called colour change boundary, determined using silver nitrate can be impacted by the pH value of the pore solution of the concrete. Research on the relationship between D_{nssm} and the pH of the pore solution in ordinary Portland cement (OPC) concrete is limited, despite its recognised significance [17–19].

Geopolymer concretes, also known as alkali-activated materials, are considered as a sustainable substitute for OPC and blended cement concretes [20]. Geopolymers are fabricated by using aluminosilicate precursors dissolved in a high alkaline solution, eliminating the usage of OPC which is carbon intensive [21, 22]. Geopolymer concretes exhibited varying pore solution pH, which may have important implications on the chloride diffusion resistance assessed using NT Build 492 [23–25]. Nevertheless, the impact of pH values on D_{nssm} of geopolymer concretes has not been investigated. The objective of this study is to examine the effect of geopolymer pore solution pH on the D_{nssm} determined using the rapid migration test (RMT)—NT Build 492. This study aims to adapt the RMT for more accurately evaluating the chloride diffusion resistance of geopolymer concretes. Moreover, this study also investigates the effects of different mix compositions on the pH of the pore solution of alkali-activated materials. The use of various components such as fly ash, ground granulated blast furnace slag (GGBFS), and calcined clay in the binder influences the pH of the pore solution. This study provides insights into the relationship between binder composition, pH values and D_{nssm} for geopolymer concretes.

2 Materials and mix design

2.1 Materials

Ground granulated blast furnace slag (GGBFS), calcined clay and two types of fly ash (FA) were utilised as the aluminosilicate precursors in this study. General Purpose (GP) cement was used for reference cement-based mix. Their chemical compositions determined by X-ray fluorescence (XRF) and particle size distribution by laser diffraction are shown in Table 1 and Fig. 1 respectively. The activator solution comprised NaOH pellets and Na-silicate solution. The sodium hydroxide (NaOH) pellets have a molecular weight of 40 g/mol, a specific gravity of 2.1 and a purity of 98%. The chemical composition of the sodium silicate solution is: 14.7% Na_2O, 29.4% SiO_2, and 55.9% H_2O. The solution has a modulus ratio (Ms) of 2, determined

Table 1 Chemical compositions of precursors

Chemical composition (wt%)	GGBFS	Eraring FA	Gladstone FA	Calcined clay	GP Cement
SiO_2	36.6	65.1	59.4	70.4	19.1
Al_2O_3	13.6	22.5	25.9	22.3	5.3
Fe_2O_3	0.5	4.2	7.7	2.3	3.0
CaO	42.3	1.8	2.6	0.5	63.7
MgO	5.9	0.7	0.8	0.2	1.1
Na_2O	0.2	0.5	0.3	0.1	0.2
K_2O	0.3	2.05	1.0	0.2	0.6
TiO_2	0.6	1.0	1.4	1.1	–
SO_3	0.5	0.1	0.1	–	2.8
Loss on ignition (LOI)	0.8	1.6	0.4	1.8	4.1

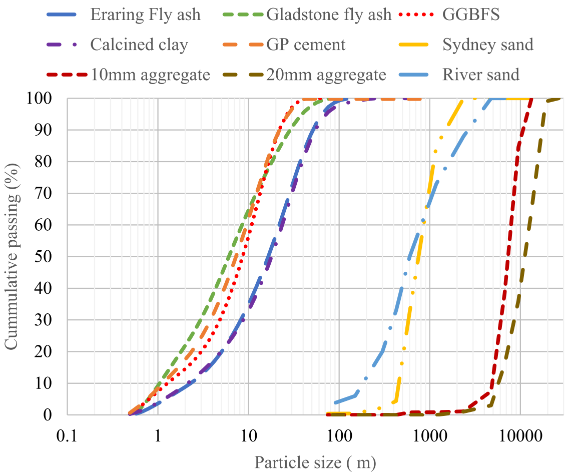

Fig. 1 Particle size distribution of precursors, GP cement and the gradation of aggregates

by the weight ratio SiO_2 to Na_2O ($SiO_2/Na_2O = 2$). Additionally, the specific gravity of the solution is 1.53 [26]. The activator solution was prepared 24 h prior to the concrete mixing. Coarse aggregate is a combination of 20 mm and 10 mm aggregates. River sand and Sydney sand were used as fine aggregate. The gradation of aggregates was shown in Fig. 1.

2.2 Mix designs

Table 2 shows the nine mix designs considered in this study. The study investigates the influence of various component compositions on the performance of geopolymer concretes through mix 1 to mix 8. Mix 9 was fabricated with 100 wt% general purpose (GP) cement for comparison purpose. The mass of the aggregate, as presented in Table 2, is in a saturated surface dry (SSD) state.

The MR (SiO_2/Na_2O) ratios, percentage of Na_2O and free water content were adjusted among the different mixes to achieve sufficient workability, setting time and compressive strength at 28 days.

2.3 Mixing and curing

In order to achieve a homogeneous dispersion, the solid constituents were initially subjected to a dry mixing process for a duration of 4.5 min, utilizing a pan mixer. The experimental procedure involved the gradual addition of an alkaline solution to the solid mixture, followed by thorough mixing for a duration of 4 min with a break of 90 s. A slump test was conducted to assess the workability of the concrete. Subsequently, freshly mixed concrete was poured into moulds and compacted using an external vibrating table to ensure adequate consolidation

Table 2 Concrete mix compositions

Materials (kg/m^3)	Mix 1	Mix 2	Mix 3	Mix 4	Mix 5	Mix 6	Mix 7	Mix 8	Mix 9
20 mm aggregate	668	615	610	612	612	610	625	617	681
10 mm aggregate	382	350	348	350	350	350	355	350	389
River sand	572	768	765	756	756	768	799	766	821
Sydney sand	287	0	0	0	0	0	0	0	0
Eraring FA	0	319	213	106	0	64	0	0	0
Gladstone FA	205	0	0	0	0	361	0	0	0
GGBFS	205	106	213	319	425	0	0	188	0
Calcined clay	0	0	0	0	0	0	375	188	0
GP cement	0	0	0	0	0	0	0	0	410
NaOH pellets	5.2	12.3	8.9	6.9	6.9	27.7	11.0	10.6	0
Na-silicate	81	195	141	108	108	172	274	224	0
Free water	136	53	120	153	153	35	48	59	185
Ms (SiO_2/Na_2O)	1.49	1.50	1.50	1.50	1.50	1.08	1.65	1.60	N/A
(SiO_2+ Na_2O)/Binder	0.10	0.22	0.16	0.13	0.13	0.23	0.34	0.29	N/A
Na_2O%/Binder	3.89	9.00	6.50	5.00	5.00	10.99	13.00	11.00	N/A
Water/Solid	0.40	0.31	0.40	0.45	0.45	0.25	0.40	0.38	0.45
GGBFS content (%)	50	25	50	75	100	0	0	50	0

and minimize the presence of entrapped air in the mixture.

Following the casting process, specimens were promptly transferred to a controlled environment for curing. After 24 h, the samples were removed from their mould. The specimens were carefully sealed to prevent moisture evaporation and stored within a controlled environment at a consistent temperature of 23 ± 2 °C until 28 days.

To measure the pH values of the pore solution of the geopolymer mixes, geopolymer paste (GPP) samples were prepared with identical compositions to geopolymer concretes without coarse and fine aggregates. The GPPs were cast into 50 × 100 mm sealed tubes. These tubes were subjected to the same sealed curing conditions at 23 ± 2 °C as the geopolymer concrete samples, allowing for a consistent and comparable experimental setup [27].

3 Methodology

3.1 Mechanical properties

The compressive strength tests were performed in accordance with the ASTM C39 standard after 28 days of sealed curing [28]. Three cylindrical specimens 100 × 200 mm for each mix design were prepared and subjected to grinding on both ends before testing.

3.2 pH measurement of pore solution

To obtain the pore solution, geopolymer paste samples were cured for a period of 28 days. The specimens underwent a compression pressure higher than 350 MPa utilizing a universal testing frame for a period of 300 s. After undergoing the process of compression, the extracted pore solution was subjected to 0.22 µm filtration. The pore solution was stored in plastic tube. The determination of the pH values was subsequently conducted utilising a calibrated pH meter [27, 29]. The pH measurement was carried out within one hour after extraction to avoid the reaction between the pore solution and external environment.

3.3 Rapid migration test—NT Build 492

The rapid migration test (RMT) was conducted according to NT Build 492 protocol [16]. The objective of this test was to determine the chloride migration coefficient under non-steady-state conditions. The experimental specimens were cylindrical concrete discs with 50 mm of thickness. These discs were extracted from the centre of three 100 × 200 mm cylindrical specimens. The experimental solutions employed in the study consisted of a catholyte solution and an anolyte solution. The catholyte solution was prepared by dissolving 10% sodium chloride (NaCl) in tap water, while the anolyte solution was prepared by dissolving 0.3 N sodium hydroxide (NaOH) in distilled water. In the experimental setup, an initial electrical potential of 30 V was applied to the specimens. Subsequently, the initial current flowing through the specimens was measured and recorded. In accordance with the guidelines by NT Build 492, various voltage values and testing durations were implemented based on the initial current. The experimental parameters, including the applied voltage, thickness of the specimens, initial and final current, and temperature, were recorded. After the testing duration, the specimens underwent a thorough rinsing process utilizing tap water to eliminate any residual testing solution. Subsequently, the specimens were divided into two separate sections along their axial plane. A freshly split segment was sprayed by a 0.1 M silver nitrate solution. Following a duration of approximately 15 min, a precipitation of white silver chloride became readily observable on the bisected surface of the specimen. In order to mitigate the influence of edge effects arising from potential leakage, measurements of chloride penetration depth were recorded at regular intervals of 10 mm, with an exclusion of the first 10 mm from each edge.

The determination of the non-steady-state chloride migration coefficient was conducted using the equation denoted as Eq. 1:

$$D_{\mathrm{nssm}} = \frac{RT}{zFE} \times \frac{x_{\mathrm{d}} - \alpha\sqrt{x_{\mathrm{d}}}}{t} \tag{1}$$

where: $E = \frac{U-2}{L}$;$\alpha = 2\sqrt{\frac{RT}{zFE}} \times \mathrm{erf}^{-1}\left(1 - \frac{2c_{\mathrm{d}}}{c_0}\right)$; $\mathrm{D}_{\mathrm{nssm}}$ is the non-steady-state chloride migration coefficient (m^2/s); z is absolute value of ion valence, for chloride, $z = 1$; F is Faraday constant, $F = 9.648 \times 10^4$ (J/(V·mol)); U is absolute value of applied voltage (V);

R is gas constant, $R = 8.314$ (J/(K·mol)); T is the average of the initial and final temperatures in the anolyte solution (°K); L is the thickness of the sample (m); x_d is the average penetration depth (m); t is the test duration (seconds); erf^{-1} is inverse of error function; c_d is chloride concentration at which the colour changes, $c_d \approx 0.07$ N for OPC concretes; c_0 is chloride concentration in the catholyte solution, $c_0 \approx 2$ N.

3.4 Measurement of chloride content at boundary colour change after chloride migration test (NT build 492)

After obtaining the average chloride penetration depth from the silver nitrate solution (Sect. 3.3), concrete discs undergone RMT without split were used for profile grinding. Every 1 mm concrete layer was powdered until the average chloride penetration depth (x_d) was reached. Acid-soluble and water-soluble chloride content of the concrete layer at the average chloride penetration depth was determined using an automatic potentiometric titration device following ASTM C1152 [30] and ASTM C1218 [31] respectively. The chloride content (C_d) at the penetration depth, i.e. colour change boundary (x_d), was interpolated using four adjacent layers.

4 Results and discussion

4.1 Mechanical properties

Figure 2 presents the compressive strength of the concretes at 28 days. Noticeably, the compressive strength of geopolymer concretes is significantly affected by the content of GGBFS. An optimal strength is observed when the GGBFS content falls within the range of 25–50%. However, as the proportion of GGBFS increases to 75% and 100%, the compressive strength values decreased. The compressive strength of mix 3 containing 50% GGBFS, 50% Eraring FA and high percentage of Na_2O shows the highest value at 53.44 MPa. In contrast, mix 5 with 100% GGBFS presents the lowest compressive strength at 38.07 MPa. Mix 6 and 7 containing 100% FA and 100% calcined clay achieved 48.82 MPa and

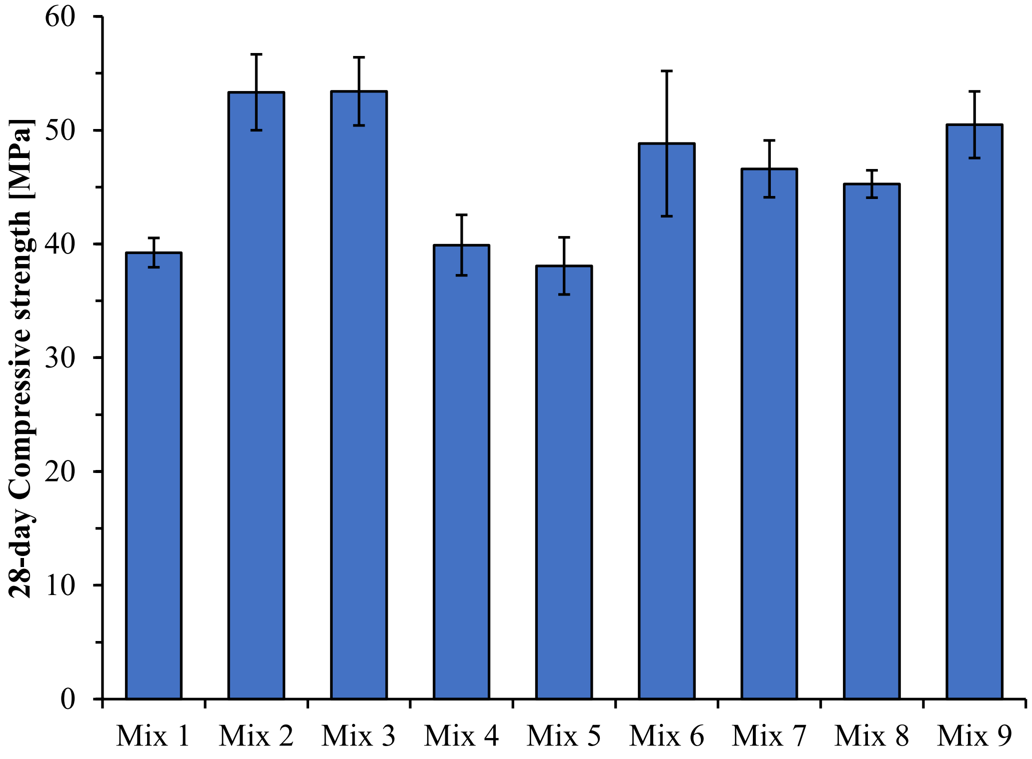

Fig. 2 Compressive strength of concrete mixes at 28 days

46.60 MPa respectively. Moreover, this finding suggests that calcined clay exhibits the capability to produce geopolymer system with suitable compressive strength under ambient curing condition, which is consistent with previous studies [22, 32]. When considering the interaction between GGBFS, fly ash, calcined clay, and the activator concentration, a wide array of compressive strengths is observed. This can be attributed to a complex and interconnected relationship among precursors and activator that collectively influence the overall strength performance of concrete.

Although the 28-day compressive strength may not be a suitable parameter for assessing the chloride diffusion resistance of geopolymer concretes [21, 33], it remains a widely used criterion for durability design in various international standards. The classification for chloride environments in accordance with Australian Standard AS 3600:2018 [34] contains four distinct exposure conditions, namely B1, B2, C1, and C2. All compressive strength results are higher than 35 MPa, indicating that the nine concrete mixes in this study fulfilled the strength requirement of B1 exposure classification to be utilised in coastal areas.

4.2 pH value of pore solution

Fig. 3 presents the pH values of the geopolymer pastes pore solution at 28 days. The pH values of all hardened geopolymers were consistently lower than that of the OPC paste (mix 9) with a pH value of 13.41. Furthermore, a general trend was observed wherein the pH of the hardened geopolymer paste exhibited an increase with increasing GGBFS content, although there was a minor reduction in mix 3. Notably, mix 5, containing 100% GGBFS, exhibited the highest pH value among all geopolymers, reaching a value of 13.30. The pH value of mix 5 was comparable to that of OPC paste (mix 9). By contrast, mix 7 with 100% calcined clay showed the lowest pH values of 12.58. Mix 7, despite having the highest Na_2O content (13%) among all concretes tested, achieved a low pH. This can be attributed to the properties of the calcined clay, which reacts differently from high-calcium precursors such as GGBFS. High Na_2O content was required for metakaolin dissolution in the calcined clay [35]. Subsequently, a significant portion of the sodium ions in the pore solutions are incorporated into the N-A-S-(H) gels, reducing the concentration of free hydroxyl ions (OH^-) necessary to maintain a high pH [22, 35]. By contrast, the presence of GGBFS produces calcium hydroxide dissolution to form C-A-S-H gels [22, 35, 36], leading to an increase in pH of the pore solution despite the lower content of Na_2O in the mix compositions.

It was found that the pH values of the pore solution in this study were higher than pH values reported in previous studies [21, 23]. This can be attributed to the method used to measure the pH. To be specific, the presence of water in the water extraction method used

Fig. 3 pH values of geopolymer pastes at 28 days

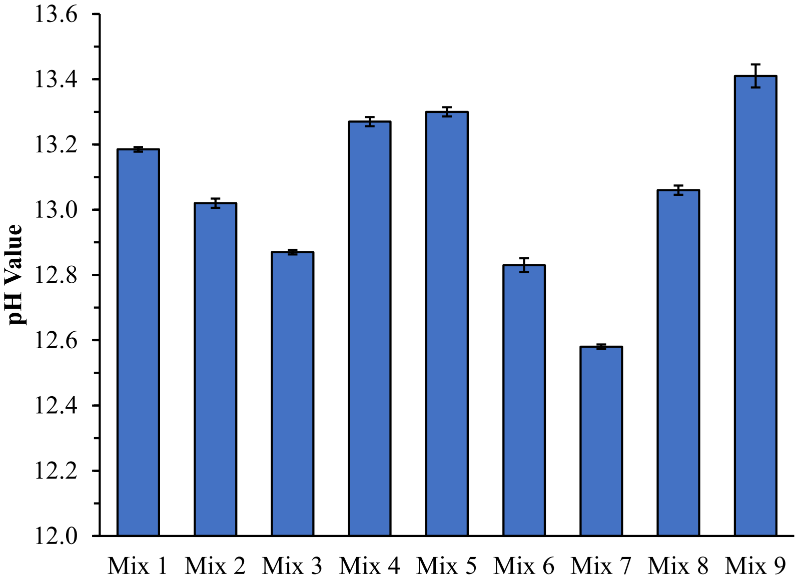

in previous studies could contribute to reduce the pH values in comparison with the direct pore solution extraction method used in this study.

According to Table 2, mix 1, mix 3, and mix 8 precursor includes 50% GGBFS content but differ in the types of fly ash and inclusion of calcined clay. Mix 1, which used Gladstone FA, has a pH value of 13.19, while mix 3 with Eraring FA has a pH value of 12.87, and mix 8 with calcined clay has a pH value of 13.06. The different types of fly ash and the inclusion of calcined clay seem to affect the pH, with Eraring FA resulting in the highest pH value and Gladstone FA the lowest within the 50% GGBFS group. Mix 4 with 75% GGBFS and mix 5 with 100% GGBFS had similar pH values of 13.27 and 13.30 respectively. These results indicate that the low-Ca precursors, such as fly ash or calcined clay, can reduce the pH of geopolymer pore solutions even with a GGBFS content up to 50%.

4.3 Chloride content at colour change boundary after rapid migration test—NT Build 492

Table 3 presents the results of the NT Build 492 test conducted on nine geopolymer concrete mixes to assess their chloride ion penetration resistance under non-steady-state conditions. The parameters measured include the applied voltage, initial and final current values, test duration, and average chloride penetration depth. The applied voltage ranged from 10V to 35V, which directly influenced the initial and final current values, as well as the chloride penetration depth. The test duration for mixes 6, 7, and 8 was limited to 6 h, which is a large reduction from the 24-h period, due to the high initial current observed in these mixes. Mixes subjected to high voltage, such as Mix 1 (35V), exhibited greater penetration depths (20.5 mm), compared to mix 5, also tested at 35V, but achieving a significantly lower penetration depth of 6.5 mm. Mix 5 contains 100% Ground Granulated Blast Furnace Slag (GGBFS). This highlights the superior resistance to chloride ingress provided by GGBFS. In contrast, Mix 7, which was composed of 100% calcined clay and tested at a lower voltage of 15V, demonstrated the greatest penetration depth of 30.9 mm, indicating a lower resistance to chloride migration, despite the shorter test duration.

Acid-soluble and water-soluble chloride content at the colour change boundary following the rapid migration test (RMT) are shown in Fig. 4. The influence of the precursor and activator concentration on the acid-soluble and water-soluble chloride contents generally agreed with the variations observed in pH values, as discussed in Sect. 4.2. For instance, for mixes with 50% GGBFS, the different fly ash and the calcined clay affected the acid-soluble and water-soluble chloride contents. In addition, the chloride binding capacity of geopolymer binders can be derived from Fig. 4. Mix 1 had an acid-soluble chloride content of 0.082% and a water-soluble chloride content at 0.078%, suggesting that 95% of the chlorides are free chloride, indicating high chloride ions mobility within the concrete matrix. Similarly, for mix 3, 98% of the chloride is free chloride. Figure 5 shows the bound chloride at the colour change boundary, obtained by the difference between acid-soluble and water-soluble chloride content (Fig. 4). In Fig. 5, Mix 2 demonstrates the highest capacity for chloride binding with a percentage of 0.016%. By contrast, mix 4 exhibits no measurable binding of chloride ions, indicating a percentage of 0%. The remaining mixes, such as Mix 6 and Mix 8, show relatively low chloride percentages of 0.001% and 0.009%, respectively. The reference OPC concrete presented 0.007% bound chloride. According to Fig. 5, the chloride binding capacity of geopolymer concrete is highly precursor composition dependent and can exceed that of the

Table 3 The data of NT Build 492 test conditions and open porosity (%) by ASTM C642

	Mix 1	Mix 2	Mix 3	Mix 4	Mix 5	Mix 6	Mix 7	Mix 8	Mix 9
Voltage (V)	35	10	25	30	35	15	10	10	20
Initial current (mA)	41.4	72.3	60.7	47.1	46.3	69.5	73.9	67.3	58.3
Final current (mA)	57.9	100.8	78.4	43.6	46.6	78	99.9	79.5	62.8
Test duration (h)	24	24	24	24	24	6	6	6	24
Average penetration depth (mm)	20.5	23.5	15.4	7.9	6.5	7	30.9	13.4	26.8
Open porosity (%)	15.03	15.09	16.75	17.29	16.99	12.46	18.11	16.52	15.16

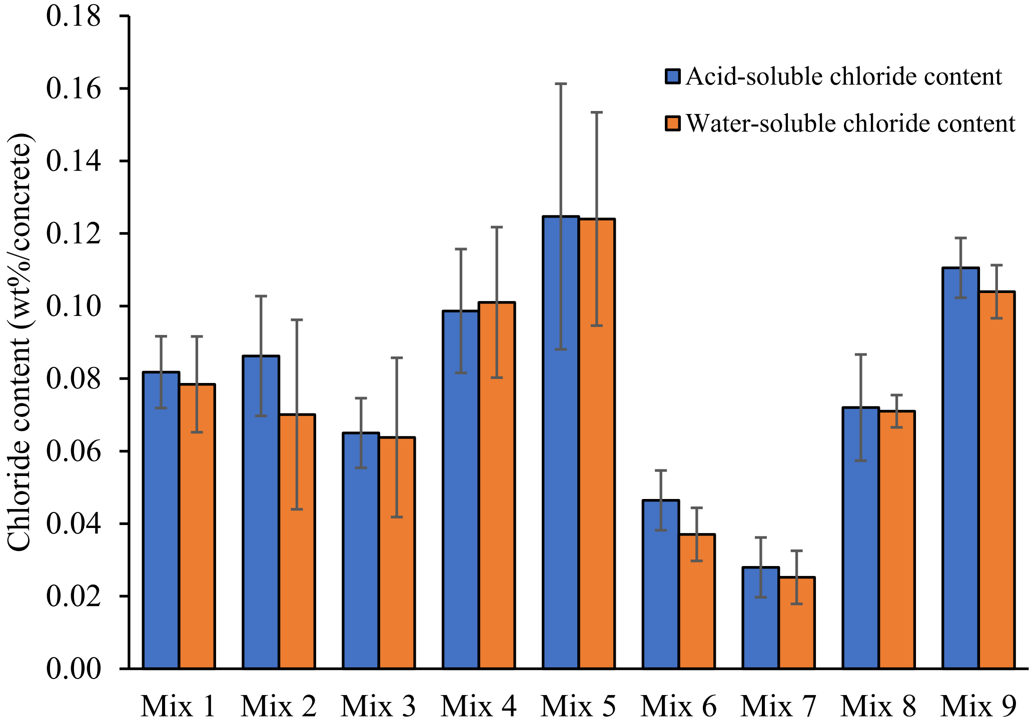

Fig. 4 Acid-soluble chloride content and Water-soluble chloride content at chloride penetration depth, i.e. colour change boundary

reference Portland cement concrete in some cases such as Mix 2 and Mix 6, both containing a large amount of Gladstone fly ash being blended or not with GGBFS.

A linear correlation between acid-soluble chloride, water-soluble chloride and pH values of the pore solution is exhibited in Fig. 6. R^2 coefficient values of approximately 0.89 and 0.88 are obtained in Fig. 6. The R^2 values indicate a strong linear correlation between the pH values of the pore solution and the concentration of acid-soluble and water-soluble chloride ions at the colour change boundary. This significant impact of the geopolymer paste pore solution pH on the chloride content at the colour change boundary must be accounted for in the calculation of the chloride migration coefficient D_{nssm} to improve the accuracy of NT Build 492 for geopolymer concrete applications (see Sect. 4.4).

4.4 Rapid migration test (RMT)—NT build 492

The determination of the non-steady-state migration coefficient (D_{nssm}) requires the consideration of various parameters as presented in Eq. (1). The chloride concentration at which the colour change (C_d) holds significant importance. The assessment of C_d parameter was conducted utilising the silver nitrate colorimetric method [37–39]. This colorimetric measurement is greatly influenced by the pH value, which represents the availability of hydroxide ions (OH^-) in the pore solution [19]. The reaction between silver ions from silver nitrate solution and free chloride ions present on the concrete results in the formation of a white precipitate known as AgCl. In contrast, the reaction between silver ions and hydroxyl ions in environments with low or no chloride ions results in the formation of Ag_2O, a brown precipitate [19]. This reaction enables the differentiation between regions that appear white and those that appear brown, thus establishing a distinct boundary. The concentration of free chloride ions (C_d) is measured at this specified boundary.

According to the NT Build 492 protocol, the C_d value of 0.07 N is recommended for OPC concretes. However, previous studies on OPC concretes have reported a notable variation in chloride content at the colour change boundary. For instance, Meck and Sirivivatnanon [40] reported an average chloride

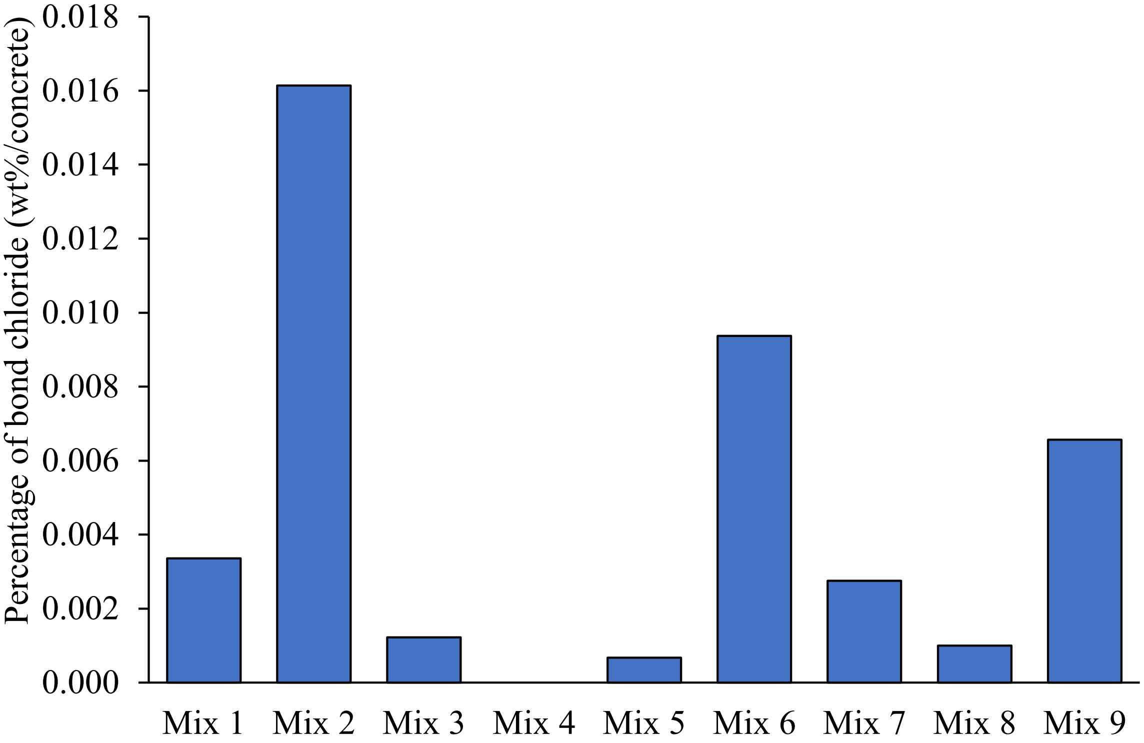

Fig. 5 Percentage of bound chloride

Fig. 6 Linear correlation between pH values of the pore solution with acid-soluble chloride content and water-soluble chloride content at colour change boundary

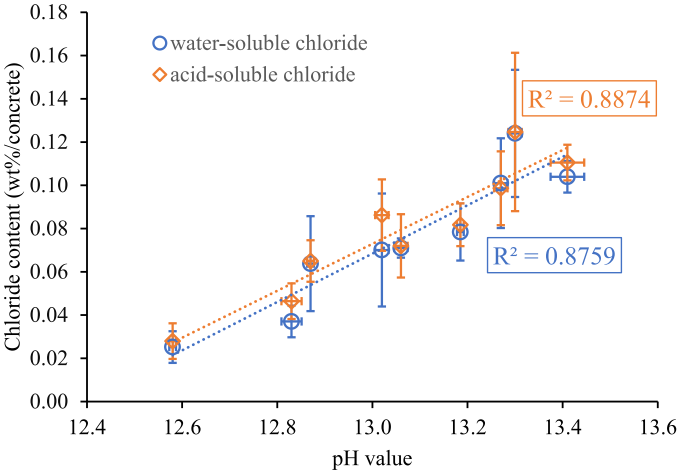

content at the colour change boundary ranging from 0.02 to 0.23% by mass of concrete whilst Andrade et al. [41] reported a chloride content at 0.18 ± 0.2% of the concrete mass. In addition, the volume of the pore solution, depending on the pore structure and porosity, was also identified as an influential factor [42]. The difference in the chemical composition of the pore solution and pore structure of geopolymer concretes compared to OPC concretes has been well-documented [24, 36, 43, 44]. Henceforth, the utilisation of the prescribed C_d value of 0.07 mol/L may lead to inaccurate D_{nssm} coefficients for geopolymer concretes.

The chloride concentration C_d (mol/L) was calculated from the free chloride content (%) by using Eq. 2 as follows [18]:

$$c_d\left({}^{mol}/_{l}\right) = \frac{\rho_{dr} \times c(\%)}{35.45 \times \varphi} \tag{2}$$

where, ρ_{dr} is the dry concrete density (kg/m^3), c (%) is free chloride content at the colour change boundary relative to the mass of the concrete, and φ is the open porosity (vol%), measured according to ASTM C642 [45]. The open porosity is determined as follows:

$$\varphi = \frac{W_a - W_d}{W_a - W_w} \tag{3}$$

where the weight of the saturated sample is denoted as W_a, the weight of the saturated sample measured under water is denoted as W_w, and the dry weight of the sample is denoted as W_d. The open porosity of each mix is presented in Table 3.

The concentration of water-soluble chloride serves as a reliable indicator of the level of free chloride present in the concrete pore solution. The free chloride content is equivalent to 80% of the water-soluble chloride content, as reported by Maes et al. [18]. The chloride concentration (mol/L) at colour change boundary calculated from the free chloride content (Eq. (2)) in this study is denoted as $C_{d\ proposed}$ (mol/L). $C_{d\ proposed}$ values for the nine mixes is presented in Fig. 7. Similar to the total and free chloride contents represented in Fig. 4, $C_{d\ proposed}$ highest value belongs to mix 5 with 100% GGBFS and the lowest value belongs to mix 7 with 100% calcined clay as the precursor.

The $C_{d\ proposed}$ for the reference OPC concrete (mix 9) was 0.35 mol/L which is consistent with a previous study [18]. The C_d value of 0.07 mol/L, adopted for Portland cement-based concrete in NT Build 492 protocol, was derived from the study of Luping Tang and Nobuaki et al. [37, 46]. The water-soluble chloride content at the colour change boundary was 0.15 wt%/binder for OPC-based concrete. In this study, the water-soluble chloride content at the colour change boundary of Mix 9 (OPC-based concrete) was 0.61 wt%/binder, leading to the $C_{d\ proposed}$ of 0.35 mol/L. The reasons for the difference in water-soluble chloride content at the colour change boundary between this study and Nobuaki et al. are unclear to the authors and require further study. However, large variations in chloride content at colour change boundary for 100% OPC-based concretes were reported in the literature, ranging from 0.28 to 0.93 wt%/binder for water-soluble chloride [40, 41], values being consistent to the 0.61 wt%/binder obtained in this study.

The $C_{d\ proposed}$ in this study showed an opposite trend to that of the chloride concentration at the colour change boundary from a previous study by Noushini et al. [21]. Specifically, increasing GGBFS content generally led to an increase in pore solution

Fig. 7 $C_{d\ proposed}$ values

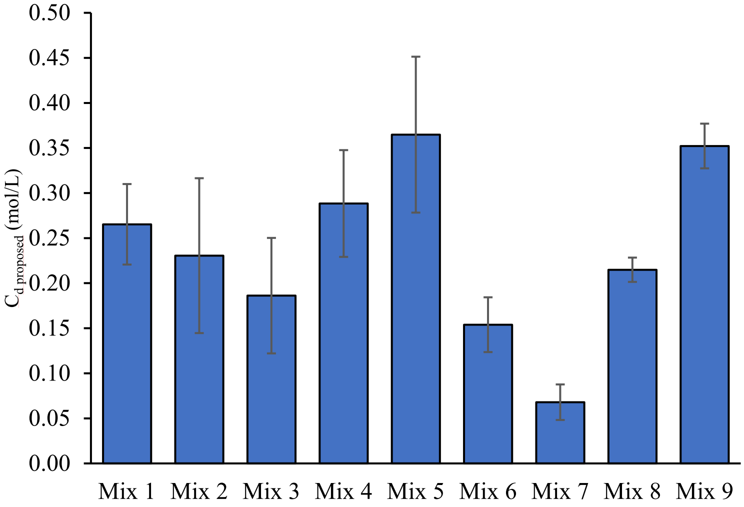

pH value and chloride concentration at the colour change boundary in this study. By contrast, Noushini et al. [21] presented a decrease in chloride concentration at the colour change boundary when increasing the GGBFS content. The difference can be explained by Noushini et al. [21] assuming that all silver nitrate is reacting with chloride and hydroxyl ions at the colour change boundary when conducting spraying test, which cannot be validated experimentally.

Figure 8 presents the relationship between open porosity and the D_{nssm} derived from the new $C_{d\ proposed}$. Figure 8 shows a weak positive relationship between porosity and the D_{nssm} values. This suggests that as porosity increases, the chloride migration coefficient D_{nssm} generally increases as well, indicating that higher porosity is associated with greater chloride permeability. However, the low R^2 value of 0.17 indicates that open porosity cannot be used to predict D_{nssm}.

The correlation between $C_{d\ proposed}$ and pH values of the pore solution is exhibited in Fig. 9. The R^2 value is very high at approximately 0.95 (Fig. 9), indicating a very strong linear correlation. The free chloride ion concentration at the colour change boundary following the RMT increases with the increase of the pH value of the pore solution. Given the strong correlation, some geopolymer concrete with high pH pore solution can present high free chloride concentration at the colour change boundary.

Table 4 presents the non-steady-state chloride migration coefficients, denoted as D_{nssm}, calculated for the nine different concretes (mix 1 to mix 9). The D_{nssm} values are determined using two different C_d values: one based on the conventional $C_d = 0.07$ and the second based on the proposed concentration $C_{d\ proposed}$ from Fig. 7. Across all concretes, the D_{nssm} values derived using $C_{d\ proposed}$ were generally lower than those obtained using C_d, except for mix 7 where both methods show similar results. The highest difference in D_{nssm} value using $C_{d\ proposed}$ compared to the conventional $C_d = 0.07$ is observed for mix 5 at 12.3%, followed by mix 8 (12.2%) and mix 4 (10.4%). Noticeably, mix 5, mix 8 and mix 4 had GGBFS contents higher than 50%. This indicates that the high slag content increasing pH values of pore solution can lead to noticeable reduction in D_{nssm} values calculated by using the $C_{d\ proposed}$ compared to conventional C_d. Mix 7 (100% calcined clay) showed no difference to $C_{d\ proposed} = 0.07$. The difference for OPC mix (mix 9) is 7.5%.

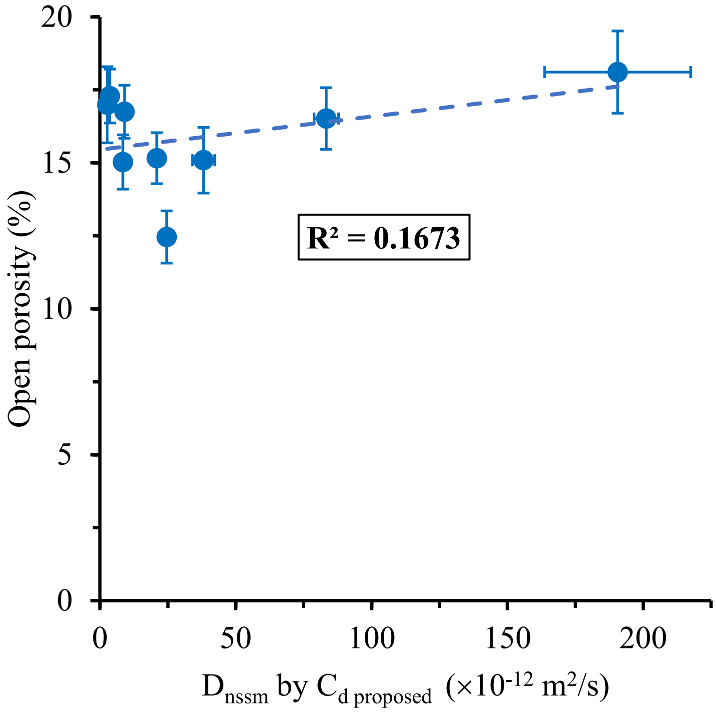

Fig. 8 Correlation of open porosity and D_{nssm} by $C_{d\ proposed}$

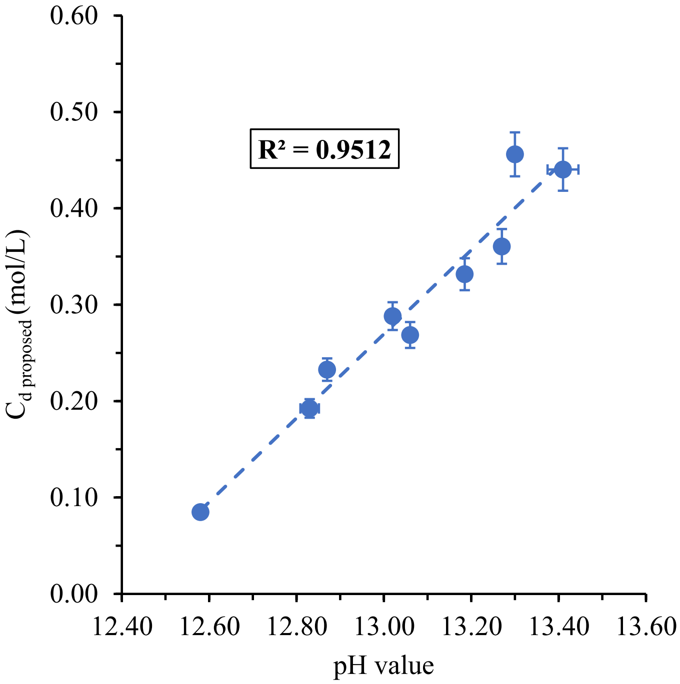

Fig. 9 Correlation of pH value and $C_{d_{proposed}}$

Table 4 D_{nssm} calculated by using $C_d = 0.07$ and $C_{d\ proposed}$ (Fig. 7)

Mix design	Mix 1	Mix 2	Mix 3	Mix 4	Mix 5	Mix 6	Mix 7	Mix 8	Mix 9
D_{nssm} by $C_{d\ proposed}$ $(\times 10^{-12}\mathrm{m}^2/s)$	8.4	38.2	9.0	3.7	2.7	24.6	190	83.3	20.9
D_{nssm} by $C_d = 0.07$ $(\times 10^{-12}\mathrm{m}^2/s)$	8.0	35.0	8.6	3.3	2.4	22.5	190	74.3	19.5
Difference of D_{nssm} (%)	4.9	9.2	4.9	10.4	12.3	9.2	0.0	12.2	7.5

5 Conclusion

This study investigates the effects of pH values from geopolymer concrete pore solution on the chloride content at the colour change boundary determined according to the standard rapid migration test (RMT)—NT Build 492. Alkali-activated concretes with wide-ranging aluminosilicate precursors, including GGBFS, fly ash and calcined clay, with variable activator concentrations were investigated. The main outcomes of this study can be summarised as follows:

- The precursor composition greatly influence the pH value of the pore solution. Concrete with 100 wt% GGBFS presented the highest pH value whilst the concrete with 100 wt% calcined clay exhibited the lowest pH value. All geopolymer concretes had the lower pH value than the 100% Portland cement-based concrete.
- Acid-soluble and water-soluble chloride contents at the colour change boundary were also depended on the concrete mix composition. Similar to the pH value, concrete with 100 wt% GGBFS and concrete with 100 wt% calcined clay displayed the highest and lowest acid-soluble and water-soluble chloride contents respectively. A linear relationship was observed between the pH value of the pore solution and the chloride content at the colour change boundary. An increasing pH value leads to an increase in both acid-soluble and water-soluble chloride content.
- The effect of the pore solution pH was implemented in the calculation of the non-steady-state migration coefficient through C_d coefficient according for the free chloride concentration at the colour change boundary.
- The non-steady-state migration (D_{nssm}) coefficient calculated using the pH depend C_d values was

higher than the D_{nssm} values calculated using the recommended $C_d = 0.07$ in NT Build 492, providing a more reasonable assessment of geopolymer concrete durability in chloride environments.

Acknowledgements The authors would like to thank the University of Technology Sydney (UTS)—Tech Lab for providing technical support.

Funding Open Access funding enabled and organized by CAUL and its Member Institutions.

Data availability statements Data will be made available on reasonable request.

Declarations

Conflict of interest The authors have no conflicts of interest to declare that are relevant to the content of this article.

References

1. Barcelo L, Kline J, Walenta G, Gartner E (2013) Cement and carbon emissions. Mater Struct 47:1055–1065
2. van Deventer JSJ, White CE, Myers RJ (2020) A roadmap for production of cement and concrete with low-CO2 emissions. Waste Biomass Valoriz 12:4745–4775
3. Miller SA, Van Roijen E, Cunningham P, Kim A (2021) Opportunities and challenges for engineering construction materials as carbon sinks. RILEM Techn Lett 6:105–118
4. Angst UM (2023) Steel corrosion in concrete—Achilles' heel for sustainable concrete? Cement Concr Res 172:107239
5. Li K, Li L (2019) Crack-altered durability properties and performance of structural concretes. Cement Concr Res 124:105811
6. Douglas Hooton R (2019) Future directions for design, specification, testing, and construction of durable concrete structures. Cement Concr Res 124:105827
7. Vaysburd AM, Emmons PH (2000) How to make today's repairs durable for tomorrow—corrosion protection in concrete repair. Constr Build Mater 14:189–197
8. Tuutti K (1982) Corrosion of steel in concrete
9. Angst UM, Geiker MR, Alonso MC, Polder R, Isgor OB, Elsener B, Wong H, Michel A, Hornbostel K, Gehlen C, François R, Sanchez M, Criado M, Sørensen H, Hansson C, Pillai R, Mundra S, Gulikers J, Raupach M, Pacheco J, Sagüés A (2019) The effect of the steel–concrete interface on chloride-induced corrosion initiation in concrete: a critical review by RILEM TC 262-SCI. Mater Struct 52:88
10. Angst U, Elsener B, Larsen CK, Vennesland Ø (2009) Critical chloride content in reinforced concrete—a review. Cement Concr Res 39:1122–1138
11. Rodriguez J, Ortega L, Casal J, Diez J (2018) Corrosion of reinforcement and service life of concrete structures. In: Durability of Building Materials and Components 7. Routledge, pp 117–126
12. Li K (2017) Durability design of concrete structures: Phenomena, modeling, and practice. John Wiley and Sons, Hoboken
13. Nguyen QD, Castel A (2023) Long-term durability of underground reinforced concrete pipes in natural chloride and carbonation environments. Constr Build Mater 394:132230
14. Glass G, Buenfeld N (2000) Chloride-induced corrosion of steel in concrete. Prog Struct Eng Mater 2:448–458
15. Bertolini L, Elsener B, Pedeferri P, Redaelli E, Polder RB (2013) Corrosion of steel in concrete: prevention, diagnosis, repair. John Wiley and Sons, Hoboken
16. NT Build 492 (1999-11) (1999) Concrete, mortar and cement-based repair materials: chloride migration coefficient from non-steady-state migration experiments, Nordtest, Espoo, Finland
17. Pontes J, Bogas JA, Real S, Silva A (2021) The rapid chloride migration test in assessing the chloride penetration resistance of normal and lightweight concrete. Appl Sci 11:7251
18. Maes M, Gruyaert E, De Belie N (2013) Resistance of concrete with blast-furnace slag against chlorides, investigated by comparing chloride profiles after migration and diffusion. Mater Struct 46:89–103
19. Yuan Q, Shi C, He F, De Schutter G, Audenaert K, Zheng K (2008) Effect of hydroxyl ions on chloride penetration depth measurement using the colorimetric method. Cement Concr Res 38:1177–1180
20. Grant Norton M, Provis JL (2020) 1000 at 1000: geopolymer technology—the current state of the art. J Mater Sci 55:13487–13489
21. Noushini A, Nguyen QD, Castel A (2021) Assessing alkali-activated concrete performance in chloride environments using NT Build 492. Mater Struct 54:57
22. Gomes SDC, Nguyen QD, Li W, Castel A (2023) Carbonation resistance of calcined clay-ground granulated blast furnace slag alkali-activated mortar. Constr Build Mater 393:131811
23. Noushini A, Castel A, Aldred J, Rawal A (2020) Chloride diffusion resistance and chloride binding capacity of fly ash-based geopolymer concrete. Cement Concr Compos 105:103290

24. Lloyd RR, Provis JL, van Deventer JSJ (2010) Pore solution composition and alkali diffusion in inorganic polymer cement. Cement Concr Res 40:1386–1392
25. Bernal SA, Provis JL, Brice DG, Kilcullen A, Duxson P, van Deventer JSJ (2012) Accelerated carbonation testing of alkali-activated binders significantly underestimates service life: the role of pore solution chemistry. Cement Concr Res 42:1317–1326
26. Noushini A, Castel A (2018) Performance-based criteria to assess the suitability of geopolymer concrete in marine environments using modified ASTM C1202 and ASTM C1556 methods. Mater Struct 51:146
27. Vollpracht A, Lothenbach B, Snellings R, Haufe J (2016) The pore solution of blended cements: a review. Mater Struct 49:3341–3367
28. ASTM C39/C39M-18 (2018) Standard test method for compressive strength of cylindrical concrete specimens. ASTM International, West Conshohocken
29. Nguyen QD, Khan MSH, Castel A (2020) Chloride diffusion in limestone flash calcined clay cement concrete. ACI Mater J 117:165
30. ASTM C1152/C1152M Standard Test Method for Acid-Soluble Chloride in Mortar and Concrete. ASTM International, West Conshohocken
31. ASTM C1218/C1218M-20 Standard Test Method for Water-Soluble Chloride in Mortar and Concrete. ASTM International, West Conshohocken
32. Tang J, Wei S, Li W, Ma S, Ji P, Shen X (2019) Synergistic effect of metakaolin and limestone on the hydration properties of Portland cement. Constr Build Mater 223:177–184
33. Tennakoon C, Shayan A, Sanjayan JG, Xu A (2017) Chloride ingress and steel corrosion in geopolymer concrete based on long term tests. Mater Des 116:287–299
34. AS 3600 (2018) Concrete structures. Standards Australia, Sydney
35. Alventosa KML, White CE (2021) The effects of calcium hydroxide and activator chemistry on alkali-activated metakaolin pastes. Cement Concr Res 145:106453
36. Zuo Y, Nedeljković M, Ye G (2019) Pore solution composition of alkali-activated slag/fly ash pastes. Cement Concr Res 115:230–250
37. Nobuaki O, Shigeyoshi N, Kenji N (1992) Evaluation of AgNO 3 solution spray method for measurement of chloride penetration into hardened cementitious matrix materials. ACI Mater J 89:587
38. He F, Shi C, Yuan Q, Chen C, Zheng K (2012) AgNO3-based colorimetric methods for measurement of chloride penetration in concrete. Constr Build Mater 26:1–8
39. Elfmarkova V, Spiesz P, Brouwers HJH (2015) Determination of the chloride diffusion coefficient in blended cement mortars. Cement Concr Res 78:190–199
40. Meck E, Sirivivatnanon V (2003) Field indicator of chloride penetration depth. Cement Concr Res 33:1113–1117
41. Andrade C, Castellote M, Alonso C, González C (1999) Relation between colourimetric chloride penetration depth and charge passed in migration tests of the type of standard ASTM C1202–91. Cement Concr Res 29:417–421
42. He F, Shi C, Yuan Q, An X, Tong B (2011) Calculation of chloride concentration at color change boundary of AgNO3 colorimetric measurement. Cement Concr Res 41:1095–1103
43. Song S, Jennings HM (1999) Pore solution chemistry of alkali-activated ground granulated blast-furnace slag. Cement Concr Res 29:159–170
44. Babaee M, Castel A (2018) Water vapor sorption isotherms, pore structure, and moisture transport characteristics of alkali-activated and Portland cement-based binders. Cement Concr Res 113:99–120
45. ASTM C642-06 Standard Test Method for Density, Absorption, and Voids in Hardened Concrete. ASTM International, West Conshohocken
46. Tang L (1996) Electrically accelerated methods for determining chloride diffusivity in concrete—current development. Mag Concr Res 48:173–179